A Novel Methodology for Optimizing Instrument Approach Procedures

Velibor Andrić, Fedja Netjasov and Miloš Nikolić
Faculty of Transport and Traffic Engineering
University of Belgrade
Belgrade, Serbia

***Abstract*—This work outlines the fundamental ideas employed to address the problem of instrument approach procedure (IAP) design using combinatorial optimization methods. Our approach takes advantage of the possibilities offered by the PBN (Performance-Based Navigation) concept, which includes structured, globally harmonized flight procedures backed by standardized performance requirements. We present a new criterion for IAP optimization, focusing on the flight crew's perspective of procedure complexity. Within this novel methodology, we have proposed a mathematical model that includes all of the essential components for generating an IAP in accordance with the specified design criteria related to the LPV (Localizer Performance with Vertical guidance) procedure. Furthermore, we have incorporated the capability to generate procedures for different landing threshold positions into the model, thereby extending the range of potential solutions. We used several generic scenarios to validate the established metaheuristic algorithm's ability to autonomously and automatically provide solutions that satisfy the specified operational requirements.**

Keywords-instrument flight procedure design; complexity; automation; optimization; metaheuristics

I. Introduction

Despite the major crises and challenges that have frightened the global economy in recent years, Europe's aviation industry has experienced a significant recovery and growth.

However, only the deployment of technological advances capable of delivering the necessary digitalization and automation in the air traffic management (ATM) sector can effectively address the existing limitations in airspace and airport capacity, which are further influenced by increased pressure from sustainability initiatives and significant regional disparities [1, 2].

The Performance-Based Navigation (PBN) concept lays the groundwork for a number of aviation initiatives, including Flexible Use of Airspace (FUA) and Free Route Airspace (FRA), which aim to address recognized constraints. The implementation of PBN principles offers advantages in terms of safety, capacity, and efficiency by allowing the flexible and harmonized development of airspace and instrument flight procedures (IFPs) that can accommodate increased traffic volumes in congested areas [3].

IFPs can play an important role in this respect since they have immense potential that has yet to be realized. As a vital component of the modern air transport system, they support air navigation throughout all phases of flight, from takeoff to landing, under diverse weather conditions, both day and night. Additionally, they guarantee the safe flying altitudes required by flight crews and air traffic controllers, which prevent collisions with ground obstacles, thereby complementing air traffic control (ATC) service and daily flight operations.

One of the primary benefits of the IFPs developed within the PBN concept is their smooth integration with other aircraft systems, particularly the Flight Management System (FMS). This allows IFPs to be systematically organized and supplied into FMS databases, permitting flight crews to load and follow complex, precise flight paths between predefined waypoints with a higher level of automation. The entire process is backed by the electronic data system, allowing continuous updates, international distribution, and implementation of navigation databases.

To ensure that potential PBN advantages are realized, a specific European Commission regulation [4] sets European-wide rules for the use of airspace and operational procedures relating to the PBN concept. This regulation foresees a complete transition to flight operations based on satellite navigation by 2030, as well as a gradual withdrawal of most of the conventional ground navigation network to limited contingency use. This transition, in addition to reducing infrastructural expenses, seeks to provide a suitable setting for optimized flight operations by enabling the development of precise and direct flight paths. The resulting consistent and predictable flight paths are expected to strengthen traffic management capabilities, increase airport capacity, and further improve air traffic safety and environmental impacts.

Furthermore, the regulation directly promotes the use of the satellite-based augmentation system (SBAS), which enables the deployment of PBN IFPs for precision approach and landing. The most recent generation of these IFPs, known as LPV (Localizer Performance with Vertical Guidance) CAT I, provides operational capabilities equivalent to current Instrument Landing System Category I (ILS CAT I) procedures. They are supported by EGNOS (European Geostationary Navigation Overlay Service), an SBAS that increases the accuracy and reliability of GNSS (Global Navigation Satellite System) signals across Europe.

LPV CAT I as an instrument approach procedure (IAP) enables aircraft to perform safe, accurate landings even in poor weather conditions without the need for ground-based navigation aids. These IAPs have the potential to significantly enhance the accessibility and operational efficiency at airports. They belong to the RNP APCH navigation specification (nav spec) based on the RNP (Required Navigation Performance) area navigation system. Nav spec is a set of performance requirements (such as accuracy, integrity, continuity, and availability) that an aircraft must meet to operate within a particular airspace or to fly a specific route.

Global aviation strategies highlight the significance of LPV CAT I procedures as key enablers of future advanced operational concepts [5, 6]. Efforts are currently being made to establish a global network of SBAS to fully utilize the potential of LPV operations [7].

The primary objective of this research is to leverage the provided framework for delivering optimal IAP solutions. We employ a comprehensive systematic approach to establish an improved automated design process that facilitates decision-making and uncovers latent capabilities in the field of procedure design. This methodology is implemented in the case of LPV CAT I procedures and can be subsequently modified for different IFPs within the PBN concept. We deliberately concentrated on IAPs as they support landing operations, the most crucial type of operations from both design and operational perspectives. Furthermore, we prioritize LPV CAT I procedures due to their exceptional operating advantages and their role as the cornerstone for future advancements.

II. Literature Overview

In the available literature, no work has been related to the LPV procedure design optimization problem. There are several studies related to IAP optimization, mainly focused on the flight path optimization problem.

This type of problem involves the optimization of a certain flight trajectory based on actual operational conditions. The problem is observed from a dynamic and real-time perspective, which is not consistent with the IAP's principal role. This role implies a predefined fixed structure capable of safely accommodating all types of traffic under the most severe anticipated operational conditions. A list of the recognized publications is included in Table I.

The principal optimization criteria in these works cover several environmental factors, predominantly centered on the RNP Authorization Required (AR) approach nav spec.

Two papers address the issue of automation of the IAP design process from an industry perspective [18, 19]. The primary difference in their methodology is the type of IAP modeled, the algorithm used for solution development, and the lack of clearly quantified optimization criteria. They concentrate on developing approach procedures with vertical guidance, which are based on the barometric altimeter, and employ an alternative algorithm type that is better suited for smaller, deterministic problems.

TABLE I. Literature Overview on the IAP Optimization

Pub.	Year	Title	Optim. Crit.	IAP Type
[8]	2023	Generation of RNP Approach Flight Procedures with an RRT* Path-Planning Algorithm	Flight Path	RNP AR APCH
[9]	2022	DRL-RNP: Deep Reinforcement Learning-Based Optimized RNP Flight Procedure Execution	Fuel Burn	RNP AR APCH
[10]	2022	RNP AR Approach Route Optimization Using a Genetic Algorithm	Flight Path	RNP AR APCH
[11]	2019	Multi-objective trajectory optimisation on environmental impacts	Noise and Emissions Level	RNAV not specified
[12]	2018	Noise mitigation optimization of A-RNP /RNP AR approaches	Noise Level	A-RNP and RNP AR APCH
[13]	2015	Optimization of Approach Trajectory Considering the Constraints Imposed on Flight Procedure Design	Fuel Burn	RNP AR APCH
[14]	2014	A Realistic Flight Path Parameterization for Calculation of Noise Minimal Trajectories using Bi-level Optimal Control	Noise Level	RNP AR APCH
[15]	2011	Development of a Multi-Event Trajectory Optimization Tool for Noise-Optimized Approach Route Design	Noise Level	RNAV with RF leg
[16]	2011	Optimization of area navigation noise abatement approach trajectories	Noise Level	RNAV 2D/3D with RF leg
[17]	2006	Framework for RNAV trajectory generation minimizing noise nuisances	Noise Level	RNAV not specified

III. IAP Design Process

This section outlines the current IAP design process based on LPV CAT I procedures considered in the research.

The IAP design process is different from that of departure, en route, or arrival procedures since it consists of five consecutive segments (four instrument and one visual), each with a specific function and distinct geometry. Each instrument approach segment is defined by two or more waypoints (WPT) and is composed of a nominal flight path and an assigned protection area [20]. Details are provided in Table II.

The WPTs and additional components used to describe the procedure for modeling purposes are (see Fig. 1):

1) IAF – Initial approach fix,
2) IF – Intermediate approach fix,
3) FAP – Final approach point,

4) DA/H – Decision altitude/height,

5) THR – Threshold,

6) MATF – Missed approach turning fix, and

7) MAEF – Missed approach end fix.

The **initial approach segment** facilitates the aircraft's transition from the en-route phase to the intermediate approach segment, which aligns with the extended runway (RWY) centerline.

The **intermediate approach segment** enables the adjustment of the aircraft's speed and configuration for landing.

The **final approach segment** facilitates the continuous descent and alignment of the aircraft for landing, and in cases where landing is not possible, it allows for the safe transition to the missed approach segment.

The **missed approach segment** allows the aircraft's positioning to initiate another approach, enter a holding procedure, or proceed to the en route phase of flight, at the specified altitude.

Flight operations are carried out along the designed approach flight path loaded from the FMS, with reference to on-board instruments and navigation display, up to the point where the DA/H is defined.

At DA/H, where altitude is referenced to mean sea level (MSL) and height to THR elevation (ELEV), the pilot in command decides whether to continue landing or initiate the missed approach part of the IAP if the required visual reference (e.g., to the THR or other available visual aids) has not been established.

Therefore, the last part of the landing phase is known as the **visual (approach) segment**, and it is not part of the optimization process in this work. The procedure configuration adopted in this research involves a basic missed approach maneuver with a straight climb or a direct fly to an MAEF with a turn at MATF.

TABLE II. LPV CAT I DESIGN CHARACTERISTICS

Start WPT	End WPT	Segment	½AW (m)	XTT (m)	ATT (m)	Max. Grad.	MOC (m)
IAF	IF	Initial App.	4630	1852	1482	8%	300
IF	FAP	Inter. App.	4630	1852	1482	3.5°	150
FAP	DA/H	Final App.	1759	556	444	3.5°	HL*
DA/H	MAEF	Missed App.	3704	1852	1482	5%	30 / 50

* Height loss value - related to the aircraft speed category.

The IAP design process consists of two iterative phases - construction and assessment. The **construction phase** includes the construction of the nominal flight path and related protection areas based on the input variables and design criteria defined in [20]. The **assessment phase** includes the assessment of the protection areas against all obstacles identified within their boundaries. As a result, a series of altitudes are established for safe navigation along the flight path. The **feasible procedure** is the one that meets all design and safety criteria and predefined operational requirements (such as airspace limitations, speed restrictions, etc.). In this work, we only consider the standard elements of the procedure.

In each iteration, a flight path is constructed from the THR using specified input values for segment track alignment (with or without a turn at IF and MATF; offset or straight-in final approach), length, and altitude at the WPT. The turns are defined as fly-by or flyover, with a minimum stabilization distance (MSD) between them. The MSD depends on the waypoint type, angle of turn (θ), aircraft speed, calculated radius of turn (r), and bank establishment time (c).

The flight path inputs are used to construct a protection area around every segment. Protection areas are statistically derived regions based on navigation system or flight data. Attributes that define protection area are area semi-width (½AW) at a waypoint and XTT, as cross-track tolerance (it is equivalent to RNP total system error (TSE)). Also, along-track tolerance (ATT) corresponds to 0.8 of the XTT value [20].

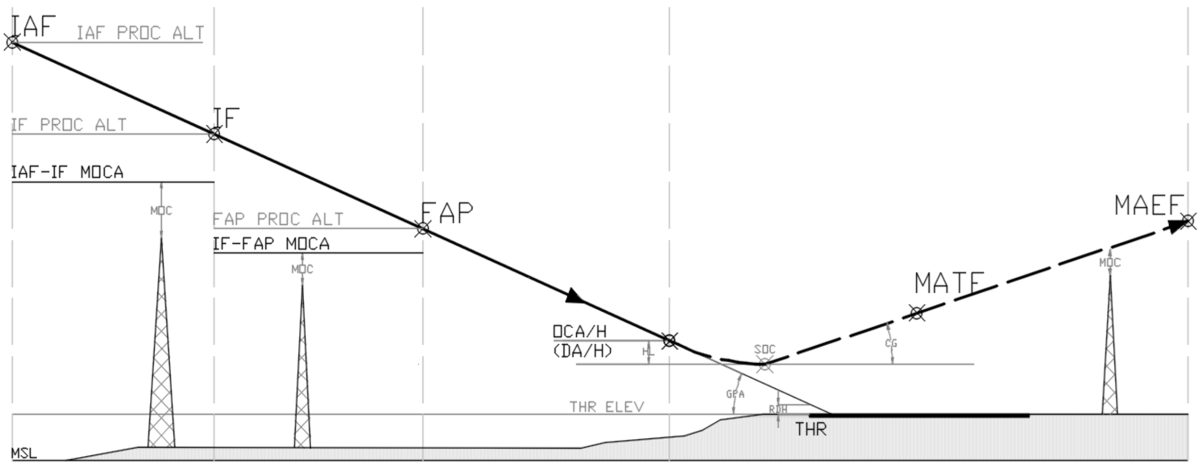

Figure 1. LPV CAT I procedure structure

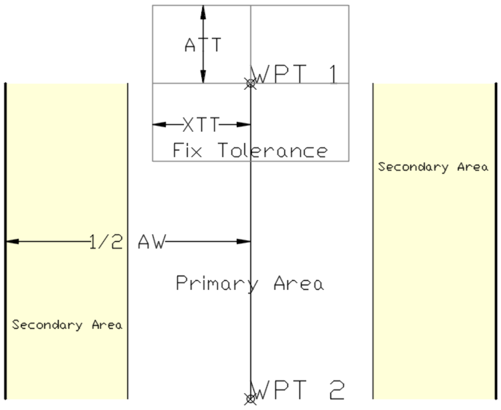

Figure 2. Protection area

The linear protection areas are related to initial, intermediate, and missed approach segments (see Fig. 2). This type of area is divided into primary and secondary parts. During the assessment phase, the full minimum obstacle clearance (MOC) value applies to obstacles in the primary area, whereas in the secondary area, this value decreases linearly to zero. Additionally, these protection areas may be designated as straight or turning areas. We employ the circular arc turn construction method for turns up to 30°, and the bounding circle method for larger turns [20].

Another type of protection area applies to the LPV CAT I final approach segment, based on the ILS CAT I obstacle assessment surfaces (OAS). The OAS consists of six sloping surfaces: W, X (left and right), Y (left and right), and Z, along with a horizontal plane. These surfaces are symmetrically arranged around the extended runway centerline and are laterally limited by a 1.9 NM-wide corridor (Fig. 3).

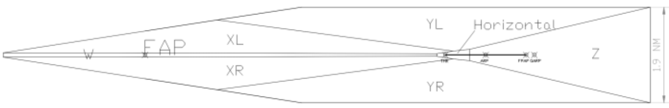

Figure 3. LPV CAT I OAS

The W surface protects the aircraft from obstacles along the final approach path, while the Z surface provides protection during a missed approach. The lateral X and Y surfaces connect W and Z on either side of the RWY centerline, and, along with the horizontal plane, form the complete OAS structure.

The geometry of the sloping surfaces is defined by linear equations with the following general form:

$$Z = A \cdot x + B \cdot y + C \tag{1}$$

The complex OAS calculation method used in this research, as described in [20, 21], begins with constructing an OAS template. This is followed by adjusting OAS constants to account for factors such as specific aircraft dimensions, aerodrome elevation, or steep glide path angles (GPA). The results are then refined to align with the LPV OAS geometry standards specified in [20].

Following the assessment phase, the primary outcomes of the design process are identified. To prevent aircraft from colliding with ground obstacles, minimum obstacle clearance altitudes (MOCAs) are determined at each WPT of the nominal flight path.

To assist flight crews in planning and executing efficient vertical profiles, procedure altitudes (PROC ALTs) are calculated based on the allowable descent gradients. Their value must be higher or equal to the associated MOCAs.

The DA/H definition incorporates an obstacle clearance altitude/height (OCA/H). The OCA/H is the result of an obstacle assessment in the final approach and the initial phase of the missed approach segment. For this research, we shall assume that DA/H equals the value of OCA/H. In practice, the aircraft operator may provide an additional operational margin.

To safely overcome the most critical obstacle in the missed approach segment, an appropriate climb gradient (CG) is established.

IV. Methodology

A. *Expansion and Automatization of the IAP Design Process*

To improve the IAP design process, we introduced a new additional output: **complexity score**. This move is motivated by expert needs and provides quantitative feedback to the procedure designer from the perspective of the flight crew, the ultimate procedure user. By regulating this criterion, decision-makers can indirectly manage the flight crew's task load, and the consequent workload imposed by the IAP, lowering the likelihood of operational errors and enhancing flight operations safety [22].

The formulation of the complexity score summarizes the deviation between the input and output variables and the optimal values for procedure construction. In the context of IAP design, the optimal values of individual elements are typically defined by design criteria or can be reasonably assumed. For instance, the lengths of critical segments, such as the intermediate and final approaches, are ideally around 5 NM. This standard may vary, but it is often established under a maximum approach speed of 250 kt, which can be considered an optimal input value for procedure development. Additionally, straight-in flight paths positively impact the complexity score, while segments involving significant turning angles tend to increase complexity. From the perspective of complexity minimization, an IAP is considered optimal when it includes maximum permissible segment lengths, avoids turns, features a straight-in approach, imposes no speed restrictions, and maintains minimal descent and climb gradients along with the lowest possible OCH.

However, the challenge lies in meeting these optimal criteria when topographical characteristics or other operational constraints make it difficult to achieve the ideal configuration. In such cases, procedure designers must deviate from some optimal elements of the IAP construction. Determining which elements to adjust and to what extent is not straightforward. To support this decision-making process, we developed a formulation that quantifies the proximity of procedure complexity to a globally optimal solution based on recognized design criteria. This formulation serves as the objective function in the optimization problem for the IAP design process. The specification of weight factors allows for the regulation of outcomes, enabling the application of tailored optimization strategies. The detailed mathematical model is presented in subsection C.

In order to facilitate the **automation** of the IAP design process, we developed supplementary features to replicate the cognitive functions of a procedure designer. These features incorporate autonomous capabilities into the design process, addressing a gap in current commercial tools, which require human intervention after each construction iteration. One such function is the deliberate increase of the OCH, which allows for the displacement of the start of the climb (SOC). This adjustment determines the earliest location of the MATF, potentially avoiding critical obstacles in the missed approach segment.

This research introduces a new capability: the simulation of THR displacement along the RWY to identify feasible alternatives (see Fig. 4). This approach significantly expands the solution space, particularly for airports in constrained locations. Additionally, by enabling the assessment of multiple runway aiming points with varying glide slopes, this capability can indirectly support the exploration of solutions with reduced noise impact.

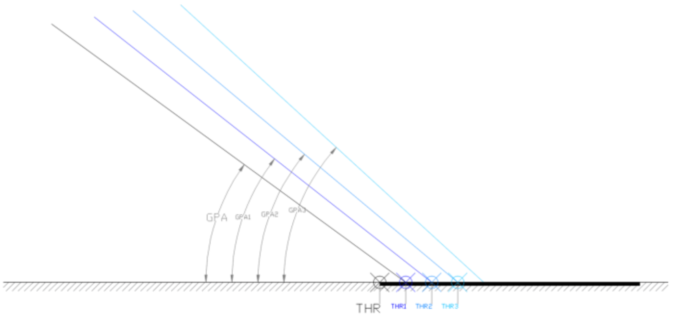

Figure 4. THR displacement

To model the complete structure of the LPV CAT I procedure, along with the added features, approximately 80 points are defined in a 3D Cartesian coordinate system. The system's origin is located at the THR, with axes ordered as X, Y, and Z. Trigonometric functions and Euclidean geometry are applied to calculate the precise coordinates of these points. These coordinates are essential for constructing the flight path and protection areas (see Fig. 5).

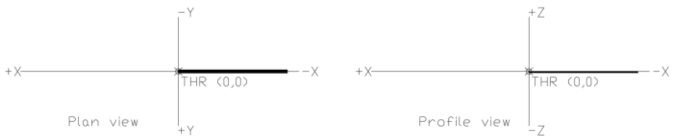

Figure 5. 3D Cartesian coordinate system

A comprehensive assessment of potential scenarios and modifications to the functions specifying the points' locations was also conducted. Additionally, a mechanism was established to identify obstacles within the defined polygons, along with a method for accurately calculating the MOC and the exact MOCAs. These tasks were carried out while addressing the complex requirements of designing the OAS and turn protection areas.

B. Problem Categorization

When the entire process of the LPV procedure design is considered, there are approximately 1.1×10^{22} possible combinations of the input variables for a single solution. This applies only when a standard procedure's charting data resolution is used. For a better resolution solution, which is sometimes necessary in obstacle-challenging conditions, the dimensions of a problem increase exponentially. Moreover, the problem is characterized by non-linear correlations between input variables as well as a lack of clear structural properties that could simplify finding a solution.

Given its dimensionality and the fact that the feasibility of the solutions is dependent on the obstacle layouts, which are unique to each airport location, IAP design is considered a **hard combinatorial optimization problem**.

C. Mathematical Model

The general minimization objective function (OF) that combines the vector of all input and output variables ($\mathbf{x}$), is defined as:

$$\min_{x \epsilon R^d} f(\mathbf{x}) = \min \left(\sum_{i=1}^{N} w_i^p \left| \frac{x_i - x_i^*}{x_i^{max} - x_i^*} \right|^p \right)^{\frac{1}{p}} \qquad (2)$$

where x_i denotes the i-th decision variable (DV) representing procedure design inputs and derived OCH value; x_i^* is the optimal DV value, and x_i^{max} is the value with the maximum (critical) divergence from the optimal one. Each DV can be seen as a separate criteria function within the search space $x \epsilon R^d$, and p represents a factor that defines the distance type ($1 \leq p < \infty$).

This formulation is based on the concept of compromise programming, which allows for calculating deviations from a known optimal or ideal solution [23]. Given the multiple DV units and diverse domains in the objective function, a normalization step was necessary to ensure uniformity and precisely measure the distance from the ideal solution. This highly adaptable formulation makes it suitable for various conditions and requirements.

The domains for each DV used in modeling an LPV procedure are shown in Table III. Each DV can take a value within the range defined by the lower (x_i^L) and upper (x_i^U) limits as specified in the design criteria. The values within this range conform to a predetermined discrete increment.

TABLE III. DV VECTOR AND DOMAINS

DV	Description	x_i^L lower limit	x_i^U upper limit	x_i^* opt.	x_i^{max} critical	Incre.
x_1	Dist. to THR	0	900	0	900	300 m
x_2	Offset app. angl.	0	±5	0	5	1°
x_3	Dist. to CP	0.4*	2.3*	2.3*	0.4*	0.1 NM
x_4	Glide path angl.	3.0	3.5	3.0	3.5	0.1°
x_5	Climb grad.	2.5	5.0	2.5	5.0	0.1%
x_6	Dist. to FAP	3.0	5.0	5.0	3.0	0.1 NM
x_7	Turn. angl. @IF	0	±90	0	90	5°
x_8	IAS @IF	185	250	250	185	5 kt
x_9	Dist. to IF	MSD+2	5.0	5.0	MSD+2	0.1 NM
x_{10}	Dist. to IAF	ATTx2	5.0	5.0	ATTx2	0.1 NM
x_{11}	OCH adjust.	0	800*	0	800*	50 ft
x_{12}	Dist. to TF	SOC+ATT	-8	-8	SOC+ATT	0.1 NM
x_{13}	Turn. angl. @TF	0	±180	0	180	5 kt
x_{14}	IAS @TF	185	250	250	185	5 kt
x_{15}	OCH	200	1000	200	1000	1 ft

± The turn side refers to the coordinate system in use: + right turn, - left turn.
* The calculation is based on a preset maximum allowable OCH value of 1000 feet.

The specified objective function is constrained by the design criteria, with conditions applied to different segment s (s ∈ {1, 2, …, N}, where N is the total number of segments):

$$L_S \geq MSD_S, \forall s \in \{1, \ldots, N\} \quad (3)$$

$$PROC\_ALT_S \geq MOCA_S, \forall s \in \{1, \ldots, K\} \quad (4)$$

$$CG_{input} \geq CG_{max}, \forall s \in \{K+1, \ldots, N\} \quad (5)$$

where L_S is the length of segment s, which must be greater than or equal to the minimum safe distance (MSD_S) for that segment. The procedure altitude ($PROC\_ALT_S$) constraint applies only to the initial and intermediate segments (from segment 1 to K) and must be at least equal to the minimum obstacle clearance altitude ($MOCA_S$). The $PROC\_ALT_S$ is applied at the initial WPT of the segment, as viewed from the THR. The climb gradient, used for protection area calculation (CG_{input}), is relevant for the missed approach segments, including final approach segment's OAS Z surface, which corresponds to segments K+1 through N. It must be greater than or equal to the CG_{max}, the value calculated for the critical identified obstacle.

D. Optimization Algorithm

Considering the provided mathematical formulation and problem characteristics, it is evident that its resolution cannot be approached from a deterministic perspective. To achieve the most effective outcomes, we disregarded methods reliant on exhaustive exploration of the solution space and concentrated on methods that allow parallel stochastic search strategies.

Our initial step involved a Bee Colony Optimization (BCO) metaheuristic algorithm. The BCO metaheuristic is a swarm intelligence algorithm where the artificial bees try to find the optimal solution to a considered combinatorial optimization problem. The artificial bees investigate a solution space similarly to how bees in nature look for food. During that process, they exchange information about the quality of the solutions they found [24].

The BCO algorithm has two versions: a constructive and an improvement. The constructive version supposes that the bees construct their solutions during each iteration, while in the improvement version, the bees are given a solution at the beginning of each iteration, and during the iteration, they are trying to improve it. To solve the considered problem in this paper, we applied the improvement version of the BCO algorithm.

The main steps of the improvement version of the BCO algorithm can be given in the following way [25]:

1. Generate initial solution
2. **do**
3.   Set the solution to all bees
4.   **for** *i* = 1 **to** *#B*
5.   Forward pass
6.   Backward pass
7.   **next**
8. **while** (stopping criteria is not satisfied)

At the beginning of the algorithm, an initial solution should be determined. For the considered problem, we determine the initial solution in a random manner, choosing one of the possible values for each variable. After that, we check the feasibility of the solution and calculate the objective function. If the solution is not feasible the objective function should be increased by some penalties.

Within the forward pass, the bees modify their solution, trying to improve them. Each bee in a random manner selects a variable whose value will be changed. After that, we check for the other variables to see if their values are feasible. If some variables do not have feasible values then, we randomly select the new values for them. When all bees modify their solutions, we calculate the new objective functions. In the backward pass, the bees exchange information and make loyalty decisions and decisions about following each other.

The backward pass can be implemented as previously described in the literature for the BCO algorithm [23, 24, 25]. Further details on implementing the BCO algorithm for this specific problem are available in our recent publication [26].

V. EXPERIMENT

To demonstrate the models' behavior and performances we created three different experiments.

In the initial experiment (**E1**), we allowed the model to generate an optimal solution in an obstacle-free environment. The optimal solution should be developed in a straightforward manner, with all optimal DV values ideally achieved in the starting iterations.

In the second experiment (**E2**), we added multiple challenging obstacles after the THR, forcing the model to develop solutions with an early turn in the missed approach segment in order to generate feasible results. The best solution should include optimal initial, intermediate, and final approach segments, as well as a shorter missed approach segment that incorporates a turn protection area near the critical obstacle.

In the final experiment (**E3**), we assessed the model's performance against additional obstacles in the approach segments prior to THR. Some of the obstacles must also be avoided due to excessive ELEV, while others are intended to verify the model's computation capabilities. The model is expected to produce the most balanced geometry across all procedure segments.

Each experiment consisted of 200 iterations. Various configurations of agents (bees) and passes (3 by 3, 5 by 5, and 10 by 10) are employed to assess the effectiveness of models in searching solution space.

A. *Settings*

The model is tested using a generic RWY with a length of 3,000 m, oriented at 09-27. Solutions are generated for RWY 09. The calculations included the following standard LPV geometry elements:

- GARP (GNSS azimuth reference point) is located 305 m after the RWY end,
- course width at THR of 210 m,
- standard dimensions of aircraft speed category D, and
- RDH (reference datum height) set at 15 m.

THR ELEV is defined at 0 m for simplified results display. The minimal PROC ALT at IAF is set at 4,000 ft and at 2,000 ft at MAEF.

The OF distance type is defined as p = 1, indicating that any deviations from the optimal solution are directly proportional to their size. Weight factors are divided into three categories based on their impact on IAP complexity:

- **High (9)** – offset approach, intermediate approach segment length and additional rising of OCH;
- **Medium (6)** – glide path angle (GPA), final approach segment length, turn angle and speed limitations at IF, distance to and speed limitations at MATF;
- **Low (3)** – THR displacement, CG, initial approach segment length, turning angle at MATF.

The OCH value is assigned greater weight (**15**) as a separate category due to its critical role in flight operations. The score of the OF configured in this manner may range from 0 to 100.

B. *Results and Discussion*

The main findings are presented in Table IV. The specific configuration of applied artificial bees, number of forward passes, and number of iterations are provided, along with the number of obstacles used, model runtime, and best OF scores achieved. Fig. 6 illustrates the best-obtained procedures in each experiment.

TABLE IV. MODEL TEST RESULTS

Exper.	Bee-Pass-Iteration	Number of Obstacles	Time per Iteration	The best OF score
E1	3 - 3 - 200	0	0.4 s	0.00
	5 - 5 - 200		1.2 s	0.00
	10 - 10 - 200		5.0 s	0.00
E2	3 - 3 - 200	5 (OBST 1-5)	1.0 s	1000.00*
	5 - 5 - 200		3.0 s	9.52
	10 - 10 - 200		13.0 s	9.52
E3	5 - 5 - 200	15 (OBST 1-15)	5.5 s	19.31

* Non-feasible solution.

TABLE V. SOLUTION VECTORS

Exper.	Solution vector with the best OF score
E1	0, 0, 2, 3, 0.025, 5, 0, 250, 5, 5, 0, -8.0, 0, 250, 200
E2	0, 0, 2, 3, 0.025, 5, 0, 250, 5, 5, 0, -8.0, 0, 250, 200
E3	0, 0, 1.1, 3, 0.030, 4, 45, 250, 4.8, 5, 0, -0.3, 60, 250, 424

TABLE VI. E3 OBSTACLE ASSESSMENT RESULTS

Segment	Obstacle	MOCA / OCH / CG_{max}	PROC ALT / OCH / CG_{input}
Initial App. (IAF-IF)	n/a	n/a	PROC ALT = 4500 ft @IAF PROC ALT = 2900 ft @IF
Inter. App. (IF-FAP)	OBST 9	MOCA = 1100 ft	PROC ALT = 1400 ft @FAP
	OBST 10	MOCA = 1000 ft	
	OBST 11	**MOCA = 1400 ft**	
	OBST 12	MOCA = 800 ft	
Final App. (OAS)	OBST 12	**OCH = 424 ft**	OCH = 424 ft
	OBST 13	n/a	
	OBST 14	OCH = 188 ft	
Initial Miss. App.	OBST 14	CG = 1.5%	CG_{input} = 3.0%
Final Miss. App.	OBST 14	CG = 1.9%	
	OBST 15	**CG = 3.0%**	

The data indicates that the model's computing efficiency declines exponentially with an increasing number of bees and passes, as well as with the volume of obstacles. The model's effectiveness in finding the optimal solutions is also confirmed by the OF scores. Table V displays the solution vectors for the best obtained solutions for each experiment.

In E1, all three configurations of the model provided the optimal solution (OF score = 0). This is also evident from the graphic representation of the generated procedure, where all segments are defined as straight and have an optimal length of 5 NM used for optimization purposes.

In E2, the second and third configurations provided the same OF score, which is in line with the presented obstacle layout. In both cases, as illustrated in Fig. 6, the generated procedure maintains optimal segment configurations prior to

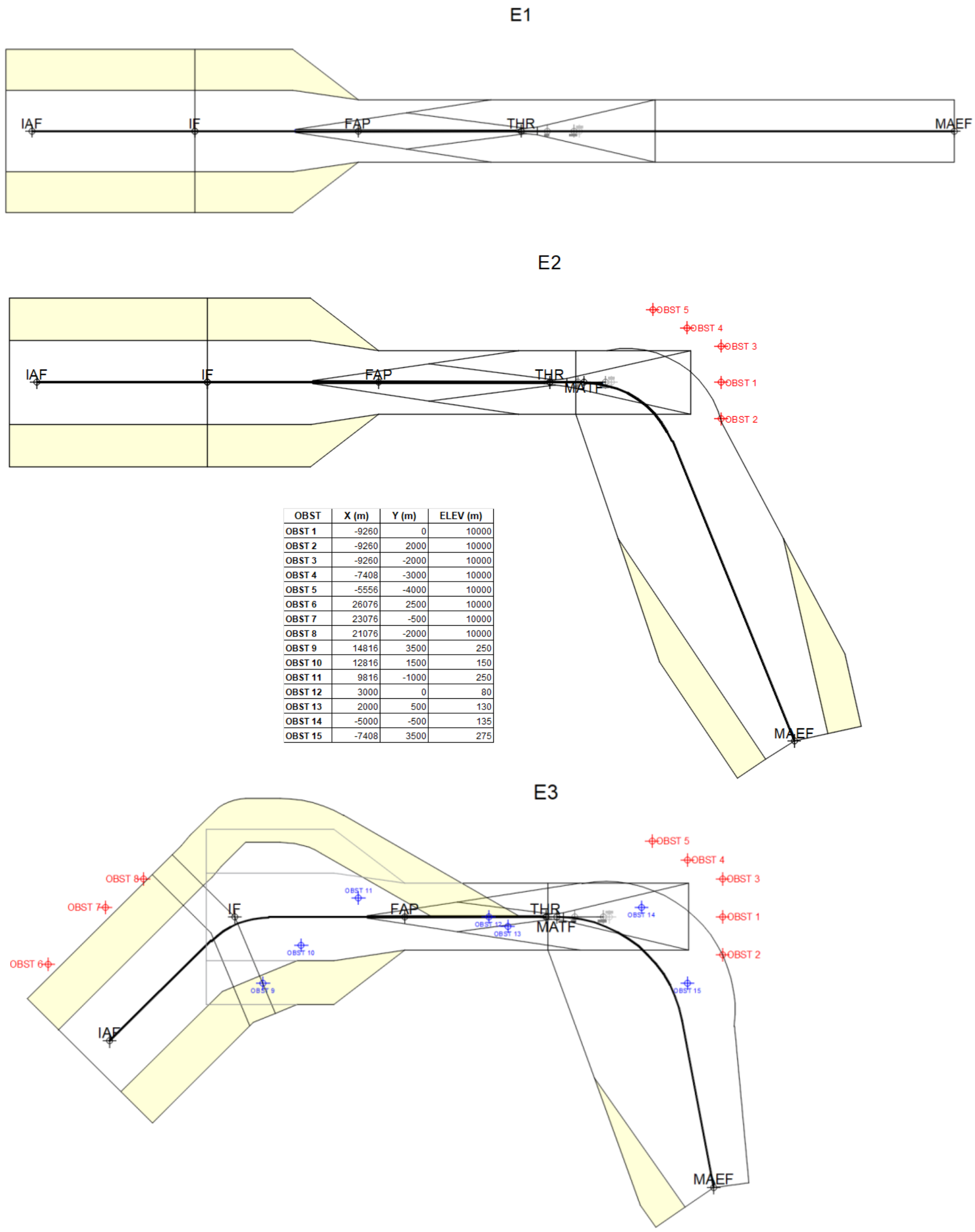

OBST	X (m)	Y (m)	ELEV (m)
OBST 1	-9260	0	10000
OBST 2	-9260	2000	10000
OBST 3	-9260	-2000	10000
OBST 4	-7408	-3000	10000
OBST 5	-5556	-4000	10000
OBST 6	26076	2500	10000
OBST 7	23076	-500	10000
OBST 8	21076	-2000	10000
OBST 9	14816	3500	250
OBST 10	12816	1500	150
OBST 11	9816	-1000	250
OBST 12	3000	0	80
OBST 13	2000	500	130
OBST 14	-5000	-500	135
OBST 15	-7408	3500	275

Figure 6. Best-generated solutions in the experiment

the THR, while the turn is introduced in the missed approach segment to avoid the high obstacles. This segment is also set to have the maximum length from THR to MATF while maintaining the turn angle to a minimum, which is consistent with the optimization criterion. However, in E2, the initial configuration, with 3 bees and 3 passes, resulted in an OF score = 1,000. This indicates that the identified solution failed to satisfy one of the model's constraints. (Each constraint violation adds 1,000 points to the OF score.) We tested this configuration multiple times, although each attempt provided unsatisfactory results. Due to the nature of stochastic algorithms, which cannot always guarantee consistent model behavior, sometimes more resources must be employed to achieve the best possible outcomes.

In E3, which features a challenging arrangement of obstacles (shown in Fig. 6) that can replicate some of the world's most difficult airport environments, we employed the middle configuration (5-5), which delivered a feasible solution within a low OF core (19.31). In this case, the model successfully configured the procedure to avoid obstacles throughout the initial and missed approach segments.

Table VI lists obstacles affecting the procedure, with rounded values for required MOCAs, OCH, and CG. The procedure generated by the model meets all requirements from the obstacle assessment phase, as shown by the consistent PROC ALT and CG input values. Several obstacles penetrated the OAS, resulting in an elevated OCH of 424 ft compared to the optimal 200 ft. Across 200 iterations, the model even explored solutions using displaced THR and offset approaches, though the final OF score was higher. Additionally, the climb gradient was raised from the standard 2.5% to 3.0%. Overall, the model met expectations, providing a solution that satisfied the specified conditions.

VI. Conclusions

The paper provides an overview of the doctoral research, expanding on the SESAR Innovation Days (SID) poster presentation from the previous year. It introduces a novel methodology for addressing the IAP optimization problem, with a particular focus on LPV CAT I procedures. While results from a real-world case study are presented in [26], the paper illustrates key insights using generic scenarios.

The proposed approach, based on a metaheuristic BCO algorithm, automates and refines the IAP design process, enabling the efficient, autonomous generation of complete approach paths that meet safety criteria. Tested across complex obstacle environments, the model has demonstrated effectiveness in optimizing procedures while adhering to design and operational requirements. Planned future enhancements aim to improve runtime efficiency and incorporate additional features, such as radius to fix (RF) turns, with further evaluation of alternative optimization algorithms.

In summary, this research offers a robust, adaptable solution for optimizing approach procedures within the evolving ATM framework.

Acknowledgment

The authors would like to thank Mr. Beat Zimmermann, the Chairman of the ICAO Instrument Flight Procedures Panel (IFPP), for providing the ICAO OAS data calculation document [9] for the academic purposes of this research.

References

[1] EUROCONTROL, European aviation in 2040, Challenges of Growth - Summary Report, Second Edition, 2018.

[2] EUROCONTROL, Aviation Outlook 2050 - Main Report, 2022.

[3] ICAO, Doc 9613 Performance-based Navigation (PBN) Manual, Fifth Edition, 2023.

[4] Commission Implementing Regulation (EU) 2018/1048 of 18 July 2018 laying down airspace usage requirements and operating procedures concerning performance-based navigation, Official Journal, L 189, pp. 3-8, 2018.

[5] SESAR 3 J, European ATM Master Plan: Digitalising Europe's aviation infrastructure – Executive view, 2020.

[6] FAA, Performance Based Navigation Strategy, 2016.

[7] J. Barrios, J. G. Pericacho, S. Domenech, and N. A. López, "Worldwide SBAS Broadcasts Between 2017 and 2022: A Comparative Study," Proceedings of the ION GNSS+ 2022, Denver, CO. pp. 117-153, 2022.

[8] R. Sáez, D. Toratani, R. Mori, and X. Prats, "Generation of RNP Approach Flight Procedures with an RRT* Path-Planning Algorithm," 2023 IEEE/AIAA 42nd Digital Avionics Systems Conference (DASC). Barcelona, Spain, 2023.

[9] L. Zhu, J. Wang, Y. Wang, Y. Ji, and J. Ren, "DRL-RNP: Deep Reinforcement Learning-Based Optimized RNP Flight Procedure Execution," Sensors, 2022, vol. 22 (17), pp. 6475.

[10] D. Toratani and R. Mori, "RNP AR Approach Route Optimization Using a Genetic Algorithm," 2022 Integrated Communication, Navigation and Surveillance Conference (ICNS), Dulles, VA, pp. 1-8, 2022.

[11] M. Zhang, Mengying, "Multi-objective trajectory optimisation on environmental impacts," PhD diss., The University of Manchester, 2019.

[12] F. Morscheck, "Noise mitigation optimization of A-RNP /RNP AR approaches," 2018 AIAA Aviation Technology, Integration, and Operations (ATIO) Conference. Atlanta, GA, 2018.

[13] T. Hasegawa, T. Tsuchiya and R. Mori, "Optimization of Approach Trajectory Considering the Constraints Imposed on Flight Procedure Design," Procedia Engineering, 2015, vol. 99, pp. 259–267.

[14] M. Richter, M. Bittner, R. M. Rieck and F. Holzapfel, "A Realistic Flight Path Parameterization for Calculation of Noise Minimal Trajectories using Bi-level Optimal Control," AIAA Guidance, Navigation, and Control Conference. National Harbor, MD, 2014.

[15] M. Braakenburg, S. Hartjes, H. Visser and S. Heblij, "Development of a Multi-Event Trajectory Optimization Tool for Noise-Optimized Approach Route Design," 11th AIAA Aviation Technology, Integration, and Operations (ATIO) Conference. Virginia Beach, VA, 2011.

[16] R. H. Hogenhuis, S. J. Hebly and H. G. Visser, "Optimization of area navigation noise abatement approach trajectories," Proceedings of the Institution of Mechanical Engineers, Part G: Journal of Aerospace Engineering, 2011, vol. 225 (5), pp.513-521.

[17] X. Prats, F. Nejjari, V. Puig, J. Quevedo, and F. Mora-Camino, "A Framework for RNAV trajectory generation minimizing noise nuisances," Proceedings of Second International Conference on Research in Air Transportation (ICRAT 2006), 2006, Belgrade, Serbia, pp. 19-28.

[18] E. Israel, W. J. Barnes, and L Smith, "Automating the Design of Instrument Flight Procedures," 2020 Integrated Communications Navigation and Surveillance Conference (ICNS), Herndon, VA, pp. IEEE. 3D2-1-3D2-11, 2020.

[19] D. Stauffer, W. J. Barnes, and L. Smith, "Modified Depth-First Search for the Automated Design of RNAV Approach Procedures," 2020 Integrated Communications Navigation and Surveillance Conference (ICNS), Herndon, VA, pp. IEEE. 3D1-1-3D1-8, 2020.

[20] ICAO, Doc 8168 Procedures for Air Navigation Services - Aircraft Operations (PANS-OPS): Volume II - Construction of Visual and Instrument Flight Procedures, Seventh Edition, 2022.

[21] NLR, Description of program booklet for the calculation of ICAO-OAS data, n.d.

[22] Y. Liu, Y. Gao, L. Yue, H. Zhang, J. Sun, and X. Wu, "A Real-Time Detection of Pilot Workload Using Low-Interference Devices." Applied Science, 2024, vol. 14 (15), pp. 6521.

[23] D. Teodorović, M. Šelmić, and T. Davidović, "Bee Colony Optimization Part II: The Application Survey," Yugoslav Journal of Operations Research, vol. 25 (2), pp. 185–219, 2015.

[24] D. Teodorović, M. Nikolić, M. Šelmić, and I. Jovanović, "Bee Colony Optimization with Applications in Transportation Engineering," vol. 1054, in Advances in Swarm Intelligence: Variations and Adaptations for Optimization Problems, A. Biswas, C. B. Kalayci and S Mirjalili, Eds. Springer Cham, 2022, pp. 135-152.

[25] M Nikolić and D. Teodorović, "Mitigation of disruptions in public transit by Bee Colony Optimization," Transportation Planning and Technology, vol. 42 (6), pp. 573-586, 2019.

[26] V. Andrić, M. Nikolić and F. Netjasov, "A metaheuristic-based optimization model for flight procedure design," Engineering Optimization, 2024.